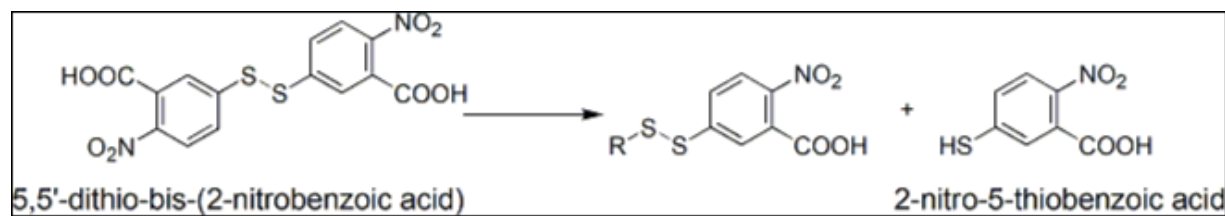
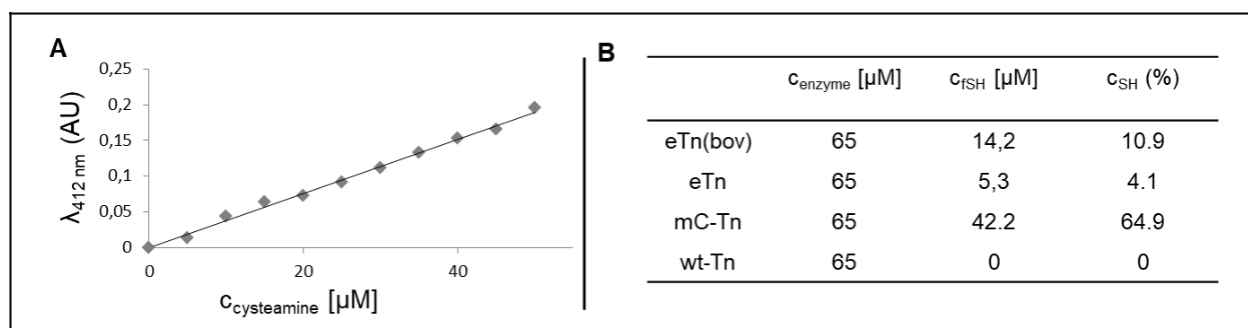


## Supplementary Tables and Figures

<b>Determination of free sulfhydryl groups</b>	<b>Figure S1</b>
<b>Calibration curve and results for the determination of free thiols</b>	<b>Figure S2</b>
<b>Non-reducing SDS-PAGE of the Tn variants</b>	<b>Figure S3</b>
<b>Hydrolysis of Bz-Arg-AMC</b>	<b>Figure S4</b>
<b>v/[S]-regression curves of Bz-Arg-AMC conversion catalyzed by diverse trypsin variants</b>	<b>Figure S5</b>
<b>Alignment of the protein sequences of anionic rat trypsin II and cationic bovine trypsin.</b>	<b>Figure S6</b>
<b>Circular dichroism (CD) measurements of bovine trypsin species</b>	<b>Figure S7</b>
<b>Thermal denaturation of aTn(bov) S195A and wt-Tn(bov) S195A measured by CD-spectroscopy</b>	<b>Figure S8</b>
<b>Sequences of the primers used for site-directed mutagenesis</b>	<b>Table S1</b>
<b>Overall structure of aTn(bov) S195A</b>	<b>Figure S9</b>
<b>Ca<sup>2+</sup>-binding site of trypsin</b>	<b>Figure S10</b>
<b>Overview of the crystallization data and refinement statistics of aTn(bov) S195A</b>	<b>Table S2</b>
<b>SDS-PAGE and mass spectrometry of trypsin variants</b>	<b>Figure S11</b>
<b>Supporting References</b>	



**Figure S1. Determination of free sulfhydryl groups.** 5,5'-Dithio-bis-(2-nitrobenzoic acid) (DTNB, ELLMAN's reagent) is used to quantify free protein thiol groups. The assay is based on the formation of colored 2-nitro-5-thiobenzoate that can be detected spectrophotometrically at 412 nm. The ELLMAN protocol was used to determine the number of free sulfhydryl groups within the Tn and Tn(bov) variants to verify the formation of the generated disulfide bond (Fig. S2) [1,2].



**Figure S2. Calibration curve and results for the determination of free thiols.** (A) Depicted is the calibration curve for determining free sulfhydryl groups using 5-50  $\mu\text{M}$  cysteamine. (B) ELLMAN's assay determines the free thiols of the trypsin species considered in this work. Conditions: 65  $\mu\text{M}$  trypsin, 0.1 mM of DTNB, 10 mM Tris/HCl buffer (pH 7.5). After incubation for 5 min at room temperature, absorbance was measured at 412 nm. Errors represent the standard deviation of three technical replicates.

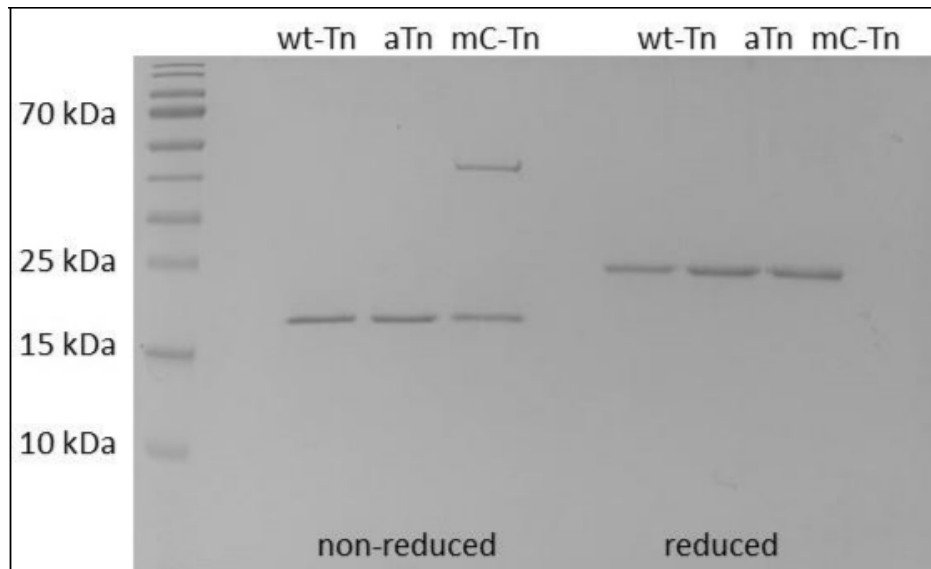


**Figure S3. Non-reducing SDS-PAGE of the Tn variants.** Shown is the electropherogram of the purified and pooled trypsin variants (wt-Tn, aTn, mC-Tn), which were either non-reduced or reduced. Conditions: 12.5% SDS-PAGE, PageRuler Prestained Protein Ladder (Promega, USA), Coomassie staining.

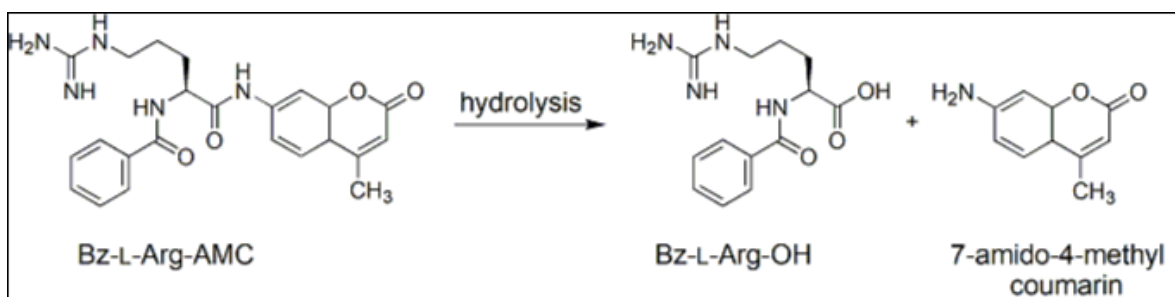


**Figure S4. Hydrolysis of Bz-Arg-AMC by trypsin.** The structures of the substrate benzoyl-L-arginine-7-amido-4-methyl coumarin (Bz-L-Arg-AMC) and the hydrolysis products benzoyl-L-arginine (Bz-L-Arg-OH) and 7-amido-4-methyl coumarin is depicted. The formation of 7-amido-4-methyl coumarin can be determined by measuring the increased fluorescence signal ( $\lambda_{\text{ex}}$  381 nm,  $\lambda_{\text{em}}$  455 nm) [3].

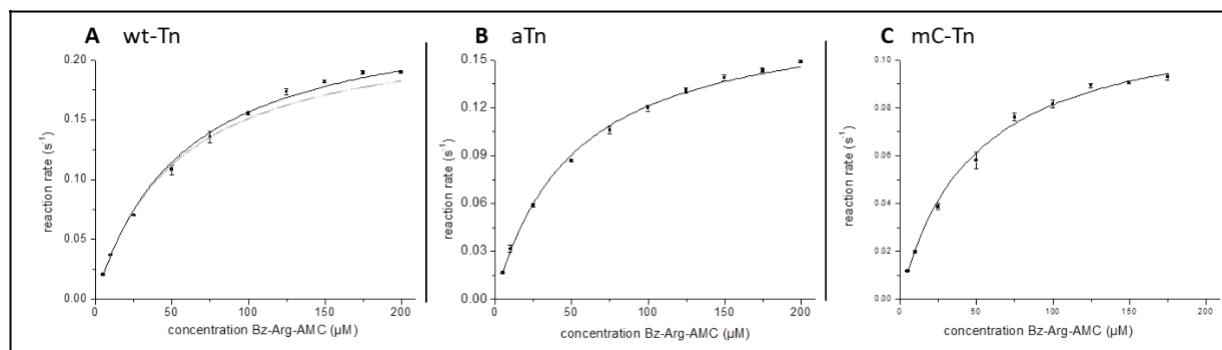


**Figure S5.  $v/[S]$ -regression curves of Bz-Arg-AMC conversion catalyzed by diverse trypsin variants.**

Depicted are the  $v/[S]$ -regression curves of the hydrolysis of Bz-Arg-AMC by wt-Tn (A), aTn (B), and mC-Tn (C). The catalytic properties of  $k_{\text{cat}}$  and  $K_M$  were determined by MICHAELIS-MENTEN regression using Origin8.1. Conditions: 16 nM Tn, 100 mM HEPES (7.8), 100 mM NaCl, 10 mM CaCl<sub>2</sub>, 1% (v/v) DMF, 5-200 μM Bz-Arg-AMC, 20 °C, measurement time 5 min,  $\lambda_{\text{ex}}$  381nm,  $\lambda_{\text{em}}$  455 nm. Errors represent the standard deviation of three technical replicates.

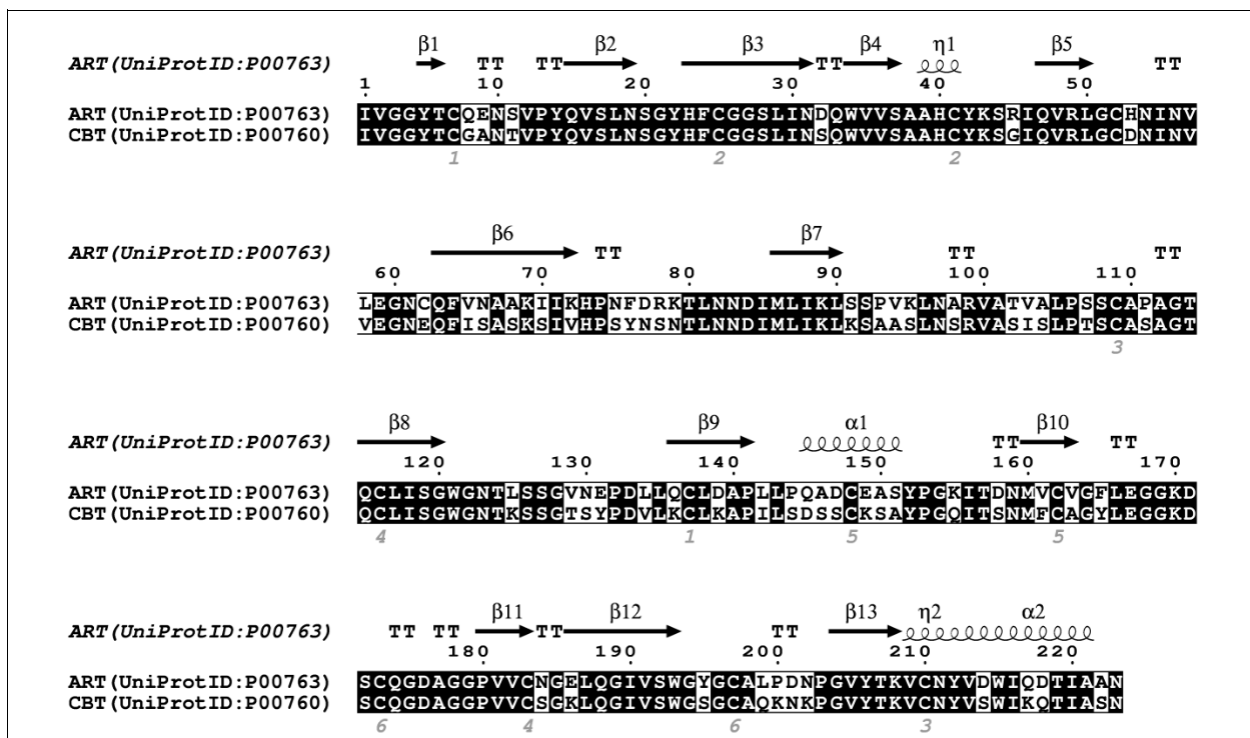


**Figure S6. Alignment of the protein sequences of anionic rat trypsin II and cationic bovine trypsin.** Shown are the aligned sequences of anionic rat trypsin (UniProtID: P00763) and cationic bovine trypsin (UniProtID: P00760) in relation to structural motifs as taken from anionic rat trypsin II (pdb-ID 1AND). Identical amino acids are marked with a black background. Structural features are labeled with  $\alpha$  ( $\alpha$ -helices),  $\eta$  ( $\eta$ -helices),  $\beta$  ( $\beta$ -sheet), TT ( $\beta$ -Turn). The alignment was performed using MultAlign and the depiction was generated with ESPript3.0 [4,5].

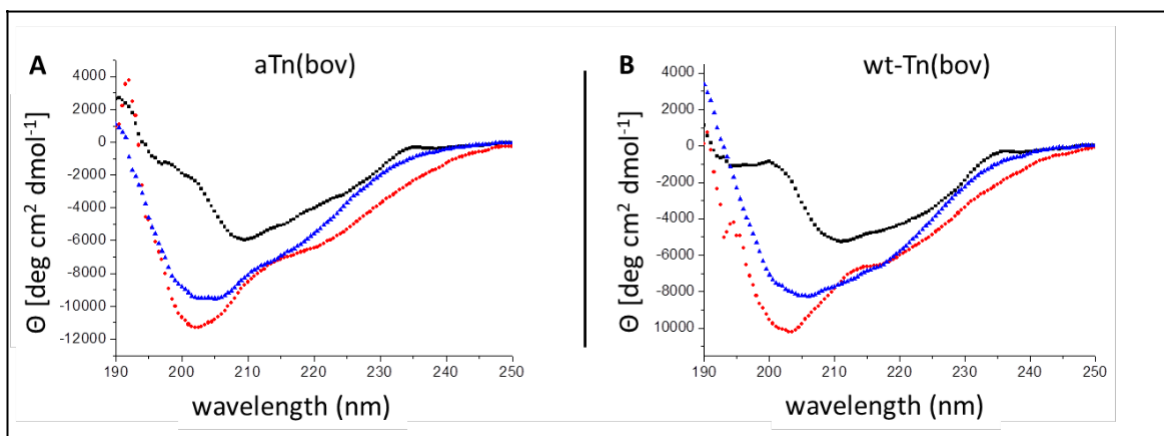


**Figure S7. Circular dichroism (CD) measurements of bovine trypsin species.** Shown are the CD-spectra of aTn(bov) (A) and wt-Tn(bov) (B) at 20 °C (black), 90 °C (red) and after cooling down from 90 °C to 20 °C (black). Tn(bov) or aTn(bov) was dissolved in 10 mM Tris/HCl buffer pH 7, 5 to a concentration of 0.1 mg ml<sup>-1</sup>. The CD spectra were recorded at the far-UV range (190-250 nm) using a 1 mm QS high precision cell cuvette and Jasco J-810 spectrometer (Jasco, Germany). All measurements were performed at either 20 °C, 90 °C, or 20 °C after heating the samples to 90 °C. Conditions: 5 μM trypsin, 10 mM Tris/HCl buffer (pH 7.5).

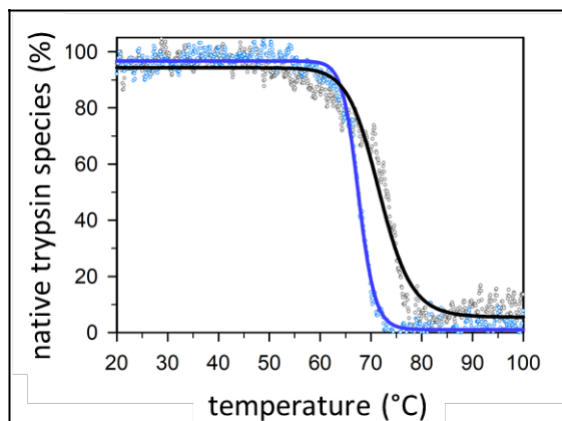


**Figure S8. Thermal denaturation of aTn(bov) S195A and wt-Tn(bov) S195A measured by CD-spectroscopy.** Due to S195A mutation, no activity measurements were possible. Instead, correct folding was verified by comparative CD spectroscopy [6]. Shown is the thermal unfolding of wt-Tn(bov) (blue) and aTn(bov) (black) monitored at 220 nm [7]. Conditions: 5 μM trypsin, 10 mM Tris/HCl buffer (pH 7.5), Slope: 1 °C min<sup>-1</sup>.

**Table S1. Sequences of the primers used for site-directed mutagenesis.** The exchanged codon/nucleotides are underlined. Variants of anionic rat trypsin II (Tn, UniProt ID: P00763) and cationic bovine trypsin (Tn(bov), Uni-Prot ID: P00760) were generated by site-directed mutagenesis based on the STRATAGENE method. All mutations were introduced using pairs of complementary primers.

	mutation		primer sequence (5' to 3')
anionic rat trypsin II	Glu70Cys	<i>for</i>	CCG CAT CCA AGT GAG ACT GGG <u>ATG TCA</u> CAA CAT CAA T
		<i>rev</i>	AAT GAT GTT GTG <u>ACA</u> TCC CAG TCT CAC TTG GAT GCG G
	Glu80Cys	<i>for</i>	GTC CTT GAG GGC AAT <u>TGT</u> CAG TTT GTC AAT GCT GCC
		<i>rev</i>	GGC AGC ATT GAC AAA CTG <u>ACA</u> ATT GCC CTG AAG GAC
cationic bovine trypsin	Glu70Cys	<i>for</i>	CAA GTG CGT CTG GGA <u>TGT</u> GAC AAC ATT AAT
		<i>rev</i>	ATT AAT GTT GTC <u>ACA</u> TCG CAG ACG CAC TTG
	Glu80Cys	<i>for</i>	GTC GTT GAG GGC AAT <u>TGC</u> CAA TTC ATC AGC
		<i>rev</i>	GCT GAT GAA TTG <u>GCA ATT</u> GCC CTC AAC ACG
	Ser195Ala	<i>for</i>	TGC CAG GGT GAC <u>GCT GGT</u> GGC CCT GTG
		<i>rev</i>	CAC AGG GCC ACC <u>AGC</u> GTC ACC CTG GCA

**Table S2. Overview of the crystallization data and refinement statistics of aTn(bov) S195A.**

Property	Value	Source
Space group	P3121	Depositor
Cell constants	57.47Å 57.47Å 105.01Å	Depositor
a, b, c, $\alpha$ , $\beta$ , $\gamma$	90.00° 90.00° 120.00°	Depositor
Resolution (Å)	49.77 – 1.40	Depositor
	44.98 – 1.40	EDS
% Data completeness	99.6 (49.77-1.40)	Depositor
(in resolution range)	99.6 (44.98-1.40)	EDS
<i>R</i> <sub>merge</sub>	(Not available)	Depositor
<i>R</i> <sub>sym</sub>	0.07	Depositor
$\langle I = \sigma(I) \rangle$	1.86 (at 1.41Å)	Xtrriage
Refinement program	REFMAC 5.8.0049	Depositor
<i>R</i> , <i>R</i> <sub>free</sub>	0.193 , 0.205	Depositor
	0.201 , 0.217	DCC
<i>R</i> <sub>free</sub> test set	1997 reflections (5.01%)	wwPDB-VP
Wilson B-factor (Å <sup>2</sup> )	16.1	Xtrriage
Anisotropy	0.049	Xtrriage
Bulk solvent <i>ksol</i> (e/Å <sup>3</sup> ), <i>Bsol</i> (Å <sup>2</sup> )	(Not available) , (Not available)	EDS
L-test for twinning	$\langle  L_j  \rangle = 0.48$ , $\langle L_2 \rangle = 0.31$	Xtrriage
Estimated twinning fraction	0.034 for -h,-k,l	Xtrriage
<i>F</i> <sub>o</sub> , <i>F</i> <sub>c</sub> correlation	0.96	EDS
Total number of atoms	1760	wwPDB-VP
Average B, all atoms (Å <sup>2</sup> )	19.0	wwPDB-VP
PDB-accession Code	8ADT	

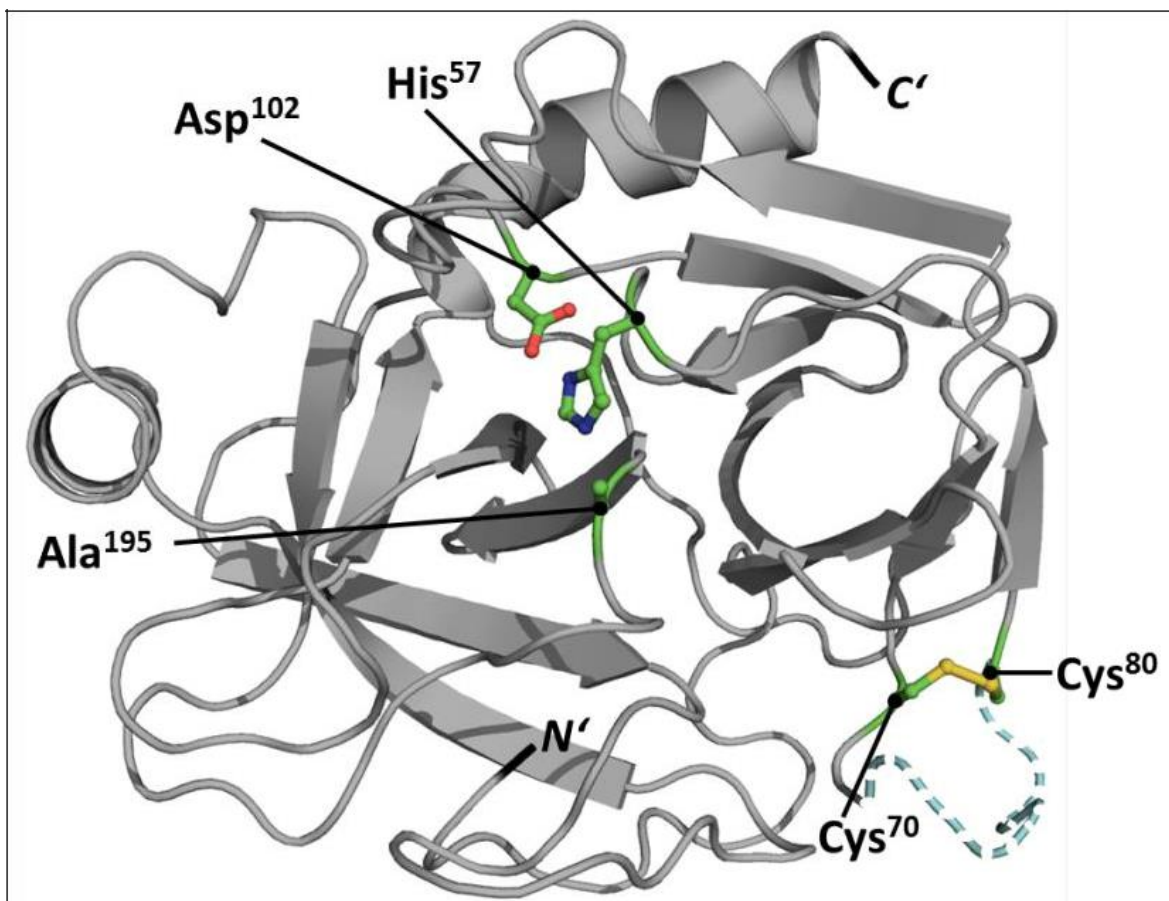


**Figure S9. Overall structure of aTn(bov) S195A.** Depicted are the overall structure of aTn(bov) (grey, cartoon) and the inactive catalytic triad consisting of Ala<sup>195</sup>, Asp<sup>102</sup>, and His<sup>57</sup> (stick form, green), as well as the generated disulfide bond consisting of Cys<sup>70</sup> and Cys<sup>80</sup> (yellow, stick form). The protein region from residue 73 to 79 couldn't be resolved via crystallization; therefore, the loop is shown in blue dots as it occurs in other cationic bovine trypsin structures (1MTS) [8].

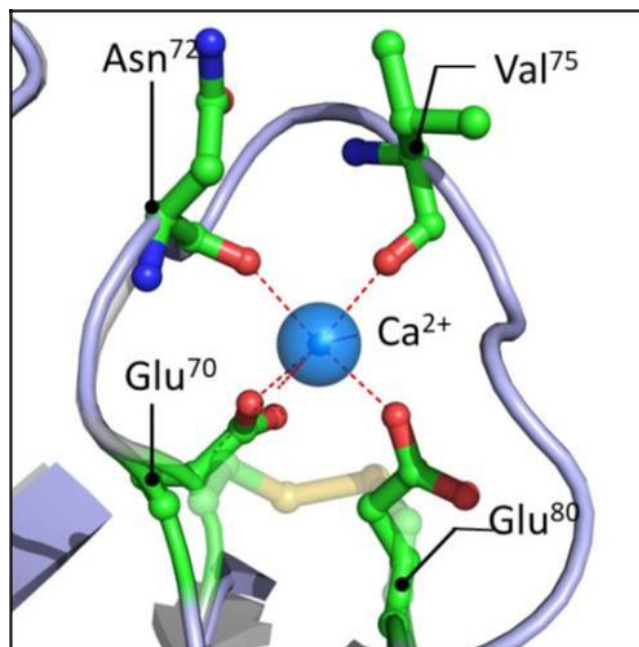


**Figure S10.  $\text{Ca}^{2+}$ -binding site of trypsin.** In anionic rat trypsin II, one  $\text{Ca}^{2+}$ -ion is located in the  $\text{Ca}^{2+}$ -binding loop (Glu70 to Glu80, blue cartoon), triggering trypsin activity [7]. In detail, the  $\text{Ca}^{2+}$ -ion (blue sphere) is coordinated by ionic interaction of the side chains of Glu70 and Glu80 (green, stick form) and a backbone interaction of Asn72 and Val75 (green, tick form). Additionally, the inserted disulfide bond is shown (transparent, stick form yellow) for better orientation purposes (pdb-code: 3TGI) [10].

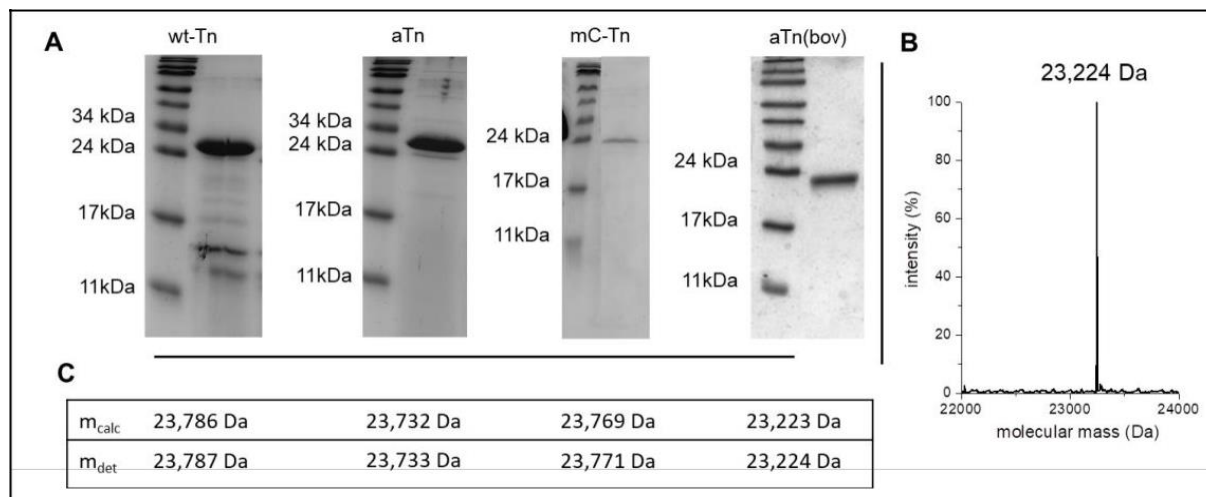


**Figure S11. SDS-PAGE and mass spectrometry of trypsin variants.** (A) Shown are the electropherograms of the purified and pooled trypsin variants. The shown samples were taken after activation for Tn variants (wt-Tn, aTn, mC-Tn). (B) The molecular mass was determined via LC-MS and calculated with MassLynx 4.1, as shown in the example of aTn(bov) ( $m_{\text{calc}}$  23,237 Da,  $m_{\text{det}}$  23,250 Da). (C) The calculated ( $m_{\text{calc}}$ ) and determined molecular mass ( $m_{\text{det}}$ ) for each trypsin variant are specified. Conditions: **A** 12.5% SDS-PAGE, PageRuler Prestained Protein Ladder (Promega, USA), Coomassie staining / **B & C** X-Bridge BEH300, linear-gradient 0 to 100% ACN (10 min), detection wavelength 254 nm, micro mass ZQ ESCI 2000 detector (Waters, USA) [11,12].

## Supporting References

1. Butterworth, P.H.; Baum, H.; Porter, J.W. A modification of the Ellman procedure for the estimation of protein sulfhydryl groups. *Arch Biochem Biophys* **1967**, *118*, 716-723.
2. Ellman, G.L. Tissue sulfhydryl groups. *Arch Biochem Biophys* **1959**, *82*, 70-77.
3. Lee, W.S.; Park, C.H.; Byun, S.M. Streptomyces griseus trypsin is stabilized against autolysis by the cooperation of a salt bridge and cation- $\pi$  interaction. *J Biochem* **2004**, *135*, 93-99.
4. Corpet, F. Multiple sequence alignment with hierarchical clustering. *Nucleic Acids Res* **1988**, *16*(22) 10881-884
5. Robert, X.; Gouet P. Deciphering key features in protein structures with the new ENDscript server. *Nucleic Acids Res* **2014** *42*(Web Server issue) W320
6. Liebscher, S.; Schopf, M.; Aumuller, T.; Sharkhuukhen, A.; Pech, A.; Hoss, E.; Parthier, C.; Jahreis, G.; Stubbs, M.T.; Bordusa, F. N-terminal protein modification by substrate-activated reverse proteolysis. *Angew Chem Int Ed Engl* **2014**, *53*, 3024-3028.
7. Sreerama, N.; Venyaminov, S.Y.; Woody, R.W. Estimation of protein secondary structure from circular dichroism spectra: inclusion of denatured proteins with native proteins in the analysis. *Anal Biochem* **2000**, *287*, 243-251.
8. Stubbs, M.T.; Huber, R.; Bode, W. Crystal structures of factor Xa specific inhibitors in complex with trypsin: structural grounds for inhibition of factor Xa and selectivity against thrombin. *FEBS Lett* **1995**, *375*, 103-107.
9. Bier, M.; Nord, F.F.; Terminiello, L. On the mechanism of enzyme action. LXI. The self digestion of trypsin, calcium-trypsin and acetyltrypsin. *Arch Biochem Biophys* **1956**, *65*, 120-131.
10. McGrath, M.E.; Haymore, B.L.; Summers, N.L.; Craik, C.S.; Fletterick, R.J. Structure of an engineered, metal-actuated switch in trypsin. *Biochemistry* **1993**, *32*, 1914-1919.
11. Laemmli, U.K. Cleavage of structural proteins during the assembly of the head of bacteriophage T4. *Nature* **1970**, *227*, 680-685.
12. Neuhoff, V.; Stamm, R.; Eibl, H. Clear Background and Highly Sensitive Protein Staining with Coomassie Blue Dyes in Polyacrylamide Gels - a Systematic Analysis. *Electrophoresis* **1985**, *6*, 427-448.